Analytical Model for Ballistic MOSFET-like Carbon Nanotube Field-Effect Transistors

Tarek M. Abdolkader
Department of Basic Sciences, Faculty of Engineering, Benha University, Egypt.
(Now with UQU, Saudi Arabia)

Esam M. Yousry
Higher Technology Institute, 10th of Ramadan, Egypt
(Now with UQU, Saudi Arabia)

Wael Fikry
Engineering Physics Department, Faculty of Engineering, Ain-Shams University, Egypt.
(Now with UQU, Saudi Arabia)

***Abstract*—An analytical model is developed for the carrier density in MOSFET-like carbon nanotube field-effect transistors in terms of surface potential. This model is based on approximating the density of states with delta function in addition to a constant value. The model has a continuous derivative and contains two fitting parameters, which are determined by best fitting with numerical results. The fitting parameters are found to depend on the subband minima and this dependence is modeled by simple quadrature formula. The model is compared to two previous analytical models with numerical results are taken as a reference and found to have less relative error. In addition, the drain current is extracted using the proposed model at various bias values. The results for current are verified by comparison with self-consistent numerical results of FETToy simulator available on the NanoHub.**

Keywords—carbon nanotube; MOSFET-like CNT transistor; compact modeling

I. INTRODUCTION

Downscaling of MOS transistors has reached its physical limits due to the degradation of device performance as a result of increasing leakage currents, and excessive short channel effects [1]. The Industry Technology Roadmap for Semiconductors (ITRS) has predicted that in the nanometer range, the CMOS devices will encounter substantial difficulties in terms of physical phenomena and technology limitations [2]. Carbon nanotube Field-Effect Transistors (CNFETs) are one of the emerging alternatives that have attracted significant attention, owing to their excellent electrical, mechanical and optoelectronic properties [3]. One of the advantages of Carbon Nanotube FETs are the high mobility of charge carriers and the potential to minimize the subthreshold swing (i.e., minimize the short channel effects) [2]. CNFETs have large mean-free-path lengths (several hundred nanometers), consequently, the transport in such devices for typical lengths is essentially ballistic [4]. It is projected that CNFET circuits can enable 5 times speed-up at the same power consumption over Si CMOS at the 11 nm technology node [5]. Therefore, according to ITRS, CNFETs are expected to replace Silicon FETs in the nano-scale by the year 2015 [6].

According to the device operation mechanism, CNFETs can be either Schottky Barrier (SB) controlled FETs or MOSFET-like FETs [6]. In SB-CNFETs, channel current is controlled by modulating the width of Schottky barrier formed between source/drain metal contacts and CNT channel. On the other hand, in MOSFET-like CNFETs, this control is made, as conventional MOSFETs, by modulating the height of the source-to-channel barrier. Some efforts have been made to explore the device characteristics of both types using either numerical simulation [3, 7, 8] or compact modeling [9-15]. This paper presents a surface potential-based compact model for the carrier density in ballistic MOSFET-like CNFETs. The model leads to the calculation of surface potential at the top of the channel barrier, and channel current for a wide range of drain and gate biases, and for various tube diameters. The model is verified by comparing results with those of FETToy numerical simulator available at the NanoHub [8].

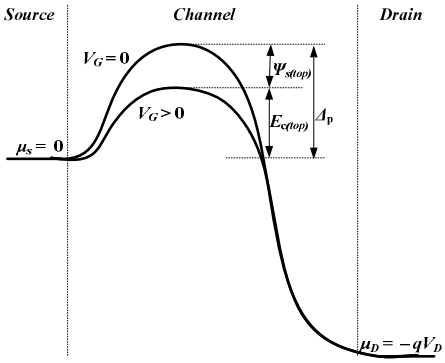

Figure 1. Energy band diagram along the channel of MOSFET-like CNFET with $V_G = 0$, and $V_G > 0$.

In Section II, the theory of ballistic 1D CNFETs is presented. The proposed model is explained in Section III, and finally results and discussion is given in Section IV.

II. THEORY OF BALLISTIC 1D CNFET

In this section, we explain the transport theory of ballistic CNFETs following the methodology given in [16]. Figure 1 shows the distribution of the conduction band minimum along the channel for an arbitrary subband. Without any gate bias ($V_G = 0$), there is a barrier to electron transport from source to drain. The height of this barrier relative to the midgap energy E_{mid} is referred as the subband minimum Δ_p, where p is a suffix

978-1-4673-6195-8/13/$31.00 ©2013 IEEE

refers to the order of the subband. Δ_p is usually modeled as [9, 12, 14],

$$\Delta_p = \Delta_1 \frac{(6p-3-(-1)^p)}{4} \quad \textbf{(1)}$$

Where $\Delta_1 = E_G/2$, and E_G is the bandgap energy.

Applying a gate bias $V_G > 0$, this barrier will be lowered by an amount equals to the surface hole potential at the top of the barrier, ψ_s. So, we can write,

$$E_{cp} = \Delta_p - \psi_s \quad \textbf{(2)}$$

With the assumption of ballistic transport over the barrier (no scattering), all +k states at the source will reach the drain and all –k states at the drain will reach the source. Moreover, with neglecting the tunneling through the barrier, the current will be determined only by how source and drain fill the states above E_{cp}.

The carrier density at the top of the barrier n_{CN} is found by summing +k states at source and –k states at the drain at energy levels above E_{cp} for all subbands. If $D(E)$ is the nanotube density of states and $f(E)$ is the Fermi-Dirac distribution function, n_{CN} can be written as,

$$n_{CN} = \sum_p \int_{E_{cp}}^{\infty} \frac{D(E)}{2}[f(E-\mu_S)+f(E-\mu_D)]dE \quad \textbf{(3)}$$

$D(E)$ is divided by 2 because at both source and drain we consider only the states in one direction. $D(E)$ is given by [4, 7, 9],

$$D(E) = D_0 \frac{(E-E_{mid})}{\sqrt{(E-E_{mid})^2-\Delta_p^2}} \quad \textbf{(4)}$$

Where $D_0 = 8/3\pi t_{CC} a_{CC}$, t_{CC} is carbon-carbon(C-C) bonding energy (≈3 eV), a_{CC} is C-C bonding distance (≈ 0.142 nm), $E_{mid} = E_{cp} - \Delta_p$, is the midgap energy. It should be noted from (2) and (3) that n_{CN} depends on ψ_s through E_{cp}.

From (3), we can see that n_{CN} is the sum of integrations of the form,

$$n_{ip} = \int_{E_{cp}}^{\infty} \frac{D(E)}{2} f(E-\mu_i)dE \quad \textbf{(5)}$$

Where $i = S$ for source, and D for drain. By replacing E by $E' + E_{cp}$, and defining the parameter ξ_{ip} as

$$\xi_{ip} = \frac{\psi_s - \Delta_p + \mu_i}{k_B T} \quad \textbf{(6)}$$

where k_B is Boltzmann constant and T is the temperature, the integration in (5) can be written as,

$$n_{ip} = \int_0^{\infty} \frac{D(E'+\Delta_p-\psi_s)}{2} f(E'-\xi_{ip})dE' \quad \textbf{(7)}$$

Further simplification can be made by defining the parameter $z = \sqrt{(E'+\Delta_p)^2-\Delta_p^2}$, so we can write,

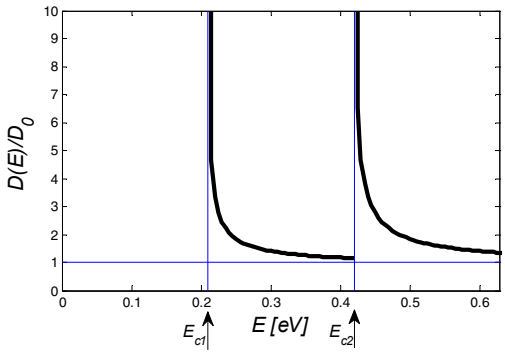

Figure 2. Relative density of states $D(E)$ in the first two subbands for a nanotube of diameter d = 2 nm.

$$n_{ip} = \frac{N_0}{k_B T} \int_0^{\infty} \frac{dz}{1+\exp\left(\frac{\sqrt{z^2+\Delta_p^2}-\Delta_p}{k_B T} - \xi_{ip}\right)} \quad \textbf{(8)}$$

where $N_0 = D_0 k_B T/2$.

On the other hand, the device electrostatics is modeled as in [16] using three model capacitances: C_G , C_D, and C_S representing channel-to-gate, channel -to-drain, and channel-to-source capacitances, respectively. Accordingly, the surface potential is related to the carrier density through,

$$\psi_s = \alpha_G V_G + \alpha_D V_D + \alpha_S V_S - q(n_{CN} - n_0)/C_{tot} \quad \textbf{(9)}$$

with $C_{tot} = C_G + C_D + C_S$, $\alpha_G = C_G/C_{tot}$, $\alpha_D = C_D/C_{tot}$, $\alpha_S = C_S/C_{tot}$, and n_0 is the carrier density at zero bias.

The transport properties of the device can be determined by the numerical solution of (8) and (9) self-consistently [8] to find ψ_s and n_{CN}. Once ψ_s is found, the drain current can be evaluated using [9-11],

$$I_D = \sum_p \ln\left[1+\exp\left(\xi_{Sp}\right)\right] - \ln\left[1+\exp\left(\xi_{Dp}\right)\right] \quad \textbf{(10)}$$

where ξ_{Sp} , ξ_{Dp} are ξ_{ip} defined by (6) evaluated at source and drain, respectively.

III. PROPOSED MODEL

Our proposed model is based on finding an approximate formula for the density of states $D(E)$ given in (4) that enables analytical solution of the integration in (7). The variation of $D(E)$ according to (4) is shown in Figure. 2 for a nanotube of diameter d = 2 nm in the first two subbands. It is noted that at energies very close to the subband minimum E_{cp}, $D(E)$ is extremely large, while at energies far above E_{cp}, it approaches a constant value D_0. Consequently, we can put $D(E)$ approximately as,

$$D(E) \simeq 2A D_0 \delta(E-E_{cp}) + B D_0 \quad \textbf{(11)}$$

where $\delta(E)$ is the delta function, A and B are fitting parameters. Now n_{ip} defined by (5) can be evaluated analytically to yield,

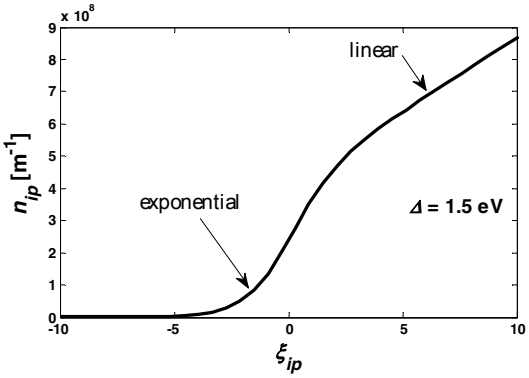

Figure 3. Carrier density integration n_{ip} versus the parameter ξ_{ip} for Δ = 1.5 eV which may correspond to the 5th subband in a tube of diameter d = 2 nm.

$$n_{ip} = A\left(\frac{D_0}{1+\exp(-\xi_{ip})}\right) + B\left(D_0 k_B T \ln\left[1+\exp(\xi_{ip})\right]\right) \qquad (12)$$

A and B are found by fitting (12) with results of numerical integration given in (8). Since n_{ip} depends only on ξ_{ip} and Δ_p, A and B are expected to depend only on the subband minimum Δ (we omit here the subscript p because it is the value of Δ that determines A and B regardless of the subband order). The dependence of A and B with Δ can be modeled by,

$$A = -0.02\Delta^2 + 0.14\Delta + 0.035 \qquad (13)$$

$$B = -0.03\Delta^2 + 0.3\Delta + 0.5 \qquad (14)$$

Figure 3 shows the variation of n_{ip} versus ξ_{ip} for both positive and negative values of ξ_{ip} calculated by (12), (13), and (14) with Δ = 1.5 eV. It should be noted that at large *positive* values of ξ_{ip}, the expression in (12) approaches a linear variation, $c_1 + c_2\,\xi_{ip}$, while at large *negative* values of ξ_{ip}, it approaches exponential variation $c_1\,\exp(\xi_{ip})$. This leads typically to the same equations of the discrete model proposed by Raychowdhury [9] separately for positive and negative values of ξ_{ip}. While the model of Raychowdhury (referred here as Model #1) has discontinuous derivative at ξ_{ip} = 0, the new proposed model given here has not. Moreover, Model #1 is limited to Δ < 0.5 eV [9], while the proposed model can be applied up to Δ = 3 eV which covers all the possible used tube diameters up to four subbands. So, the new proposed model is not limited to V_G < 500 mV, but rather valid for larger values of V_G. Some other model (referred here as Model #2) was given [11, 17], which used interpolation function to remove discontinuity in Model #1 but on the expense of giving up some of model accuracy. Comparison of the proposed model and the previous two models will be shown in the next section. The continuity of the model leads to a compact model for quantum capacitance (derivative of charge with potential).

IV. Results and Discussion

A comparison between the value of n_{ip} of the proposed model and that of numerical integration is given in Fig. 4 for two values of Δ (0.25 and 0.5 eV) with the results of the two previous models are also shown. The values of Δ are chosen to be not more than 0.5 eV which is the range of validity of the

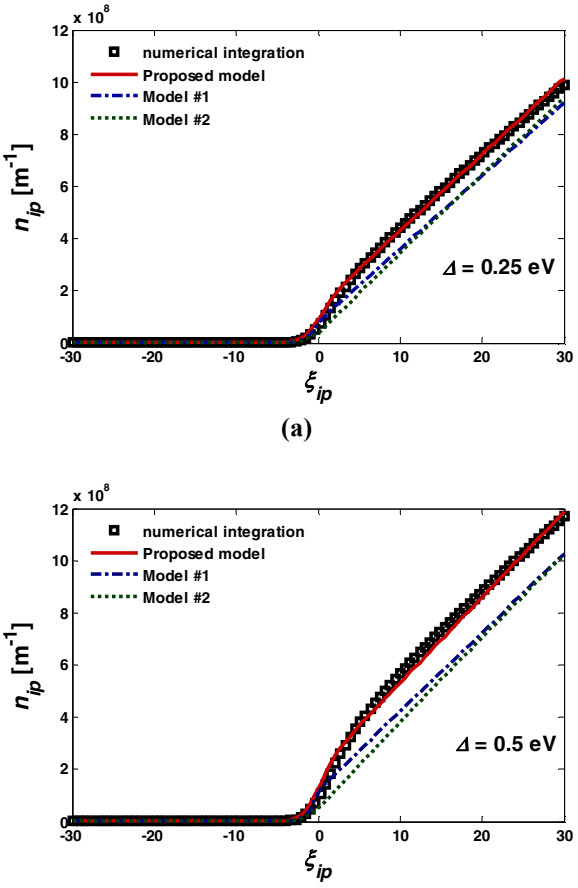

Figure 4. Carrier density integration n_{ip} versus the parameter ξ_{ip} for (a) Δ = 0.25 eV and (b) Δ = 0.5 eV. Results are given using the proposed model compared with previous models with numerical results as a reference.

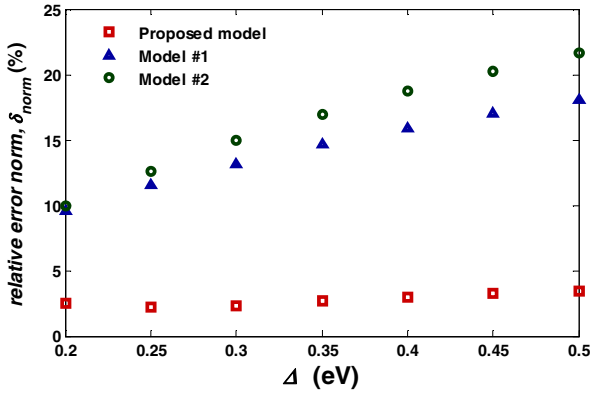

Figure 5. Relative error norm in n_{ip} calculation using proposed model (squares), Model #1 (triangles), and Model #2 (circles). The largest error happens at Δ = 0.5 eV and equals 3.5% for the proposed model.

previous models [9]. The range of ξ_{ip} includes negative and positive values between –30 and 30. To assess the accuracy of the proposed model we define δ_{norm} as the ratio of the norm of the error along the whole range of ξ_{ip} to the norm of n_{ip} values calculated numerically. δ_{norm} is shown in Fig. 5 for different values of Δ from 0.2 eV to 0.5 eV. The greatest error norm in this range is at Δ = 0.5 eV and equals 3.5% for the proposed model. For the other two models, it is 18.1% for Model #1 and 21.7% for Model #2. If we consider only the first subband, the

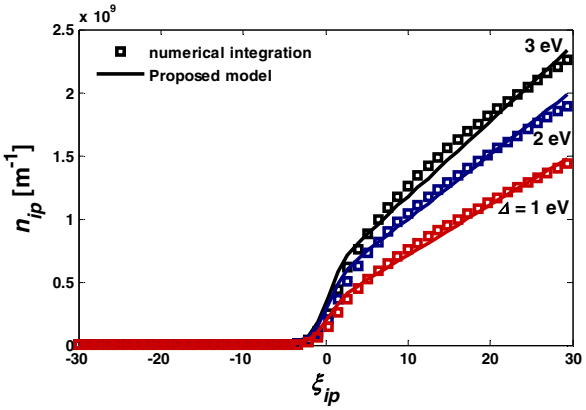

Figure 6. Carrier density integration n_{ip} versus the parameter ξ_{ip} calculated by both numerical integration (markers) and proposed model (solid line), for $\Delta = 1$, 2 and $\Delta = 3$ eV.

above range of Δ (0.2 – 0.5 eV) will span all diameters between 0.84 and 2.1 nm, which may be practically adequate. However, for higher values of V_G, where the higher subbands are important, Δ may be up to 3 eV. A comparison between proposed model and numerical results is shown in Fig. 6, but now for values of Δ exceeding 0.5 eV (1, 2, and 3 eV). The relative norm error, δ_{norm} is 4%, 4.5%, and 4.8% for $\Delta = 1$, 2, and 3 eV, respectively.

The model equation (12) can be used with (9) to solve for the carrier density integration n_{ip} and the surface potential ψ_S. Hence, the carrier density at the top of the barrier n_{CN} is found by summing n_{ip}, and the drain current I_D could be found using (10). The results are, then, compared to FETToy simulator [8] available on the NanoHub. The gate-insulator thickness is chosen as 1.5 nm, and the model capacitances C_G, C_D, and C_S used in (9) are chosen such that the parameters $\alpha_G = 0.88$ and $\alpha_D = 0.035$. Four subbands are considered in the solution. In Fig. 7, the total carrier density n_{CN} is plotted versus the gate bias V_G at $V_D = 0.1$ V for three different diameters 1.02, 2.19, and 3.13 nm. Markers represent FETToy results while solid lines represent model results. It is noted from the figure that good agreement with FETToy is maintained for a large range of V_G up to 2V. The I_D -V_G characteristics evaluated using model is compared with FETToy simulator and shown in Fig. 8. The tube diameter is chosen as $d = 1.96$ nm. The dependence of I_D on the drain bias V_D is weak, especially for $V_G < 1$V. I_D - V_D characteristics are shown in Fig. 9 for the same diameter and for $V_G = 0.2, 0.4, \ldots, 1$ V.

V. Conclusion

A physics-based analytical model is proposed for the carrier density in MOSFET-like Carbon Nanotube Field-Effect Transistors (CNFETs). The model has continuous derivative and contains two fitting parameters. The results of the model are compared with two previous analytical models taking the numerical results as a reference. Less relative error norm (up to 3.5% compared to 18.1 and 21.7% for previous models) and larger range of validity (up to 3 eV subband minimum compared to 0.5 eV for previous models) are recorded for the proposed model. By extending the range of validity to 3 eV, the model can take more subbands into consideration for most practical tube diameters. Furthermore, I_D -V_G and I_D -V_D characteristics are calculated using the model and verified by comparing with FETToy simulator results.

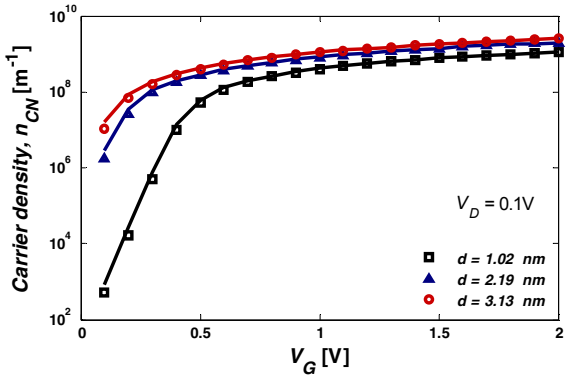

Figure 7. Total carrier density at the top of the barrier n_{CN} versus gate bias for three different tube diameters d = 1.02, 2.19 and 3.13 nm. Markers represent FETToy simulator results while solid lines represent proposed model results. V_D is fixed at 0.1V.

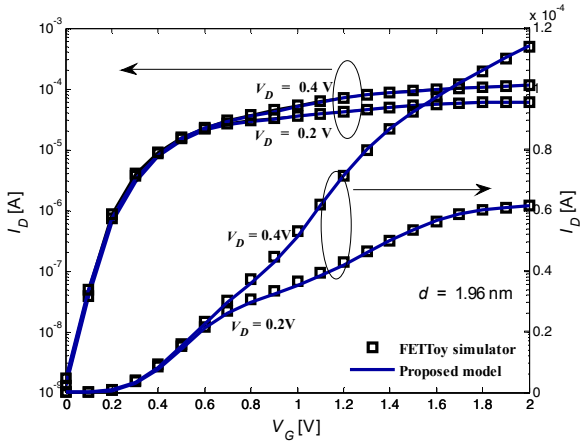

Figure 8. I_D - V_G characteristics calculated by FETToy simulator (markers) and proposed model (solid line), for $V_D = 0.2$ and *0.4* V. The diameter is chosen to be 1.96 nm.

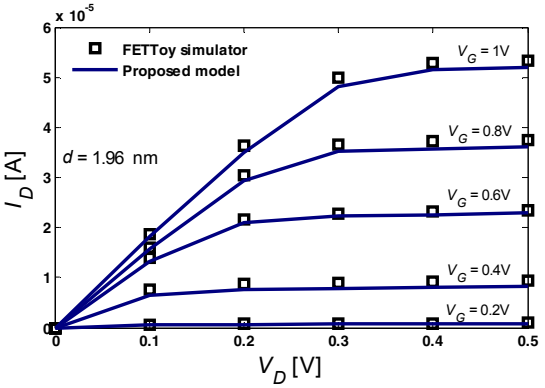

Figure 9. I_D - V_D characteristics calculated by FETToy simulator (markers) and proposed model (solid line), for $V_G = 0.2, 0.4, \ldots, 1$ V. The diameter is chosen to be 1.96 nm.

References

[1] U. Schwalke, *et al.*, "Nanoelectronics: From silicon to graphene," in *Design & Technology of Integrated Systems in Nanoscale Era (DTIS), 2012 7th International Conference on*, pp. 1-3, 2012.

[2] S. I. Association, "*International Technology Roadmap for Semiconductors*," 2011, http://www.itrs.net/.

[3] T. M. Abdolkader and M. A. Alam, "Efficient Multi-Scale Self-Consistent Simulation of Planar Schottky-Barrier Carbon Nanotube Field-Effect Transistors and Arrays," in *Micro/Nano Symposium (UGIM), 2010 18th Biennial University/Government/Industry*, pp. 1-5, 2010.

[4] M. S. Lundstrom and J. Guo, *NANOSCALE TRANSISTORS: Device Physics, Modeling and Simulation*: Springer, 2010.

[5] H. S. P. Wong, *et al.*, "Carbon nanotube electronics - Materials, devices, circuits, design, modeling, and performance projection," in *Electron Devices Meeting (IEDM), 2011 IEEE International*, pp. 23.1.1-23.1.4, 2011.

[6] S. M. K. Bari, *et al.*, "Design and Performance Analysis of Ultra Fast CNFET Comparator and CMOS Implementation Comparison," in *Computer Modelling and Simulation (UKSim), 2012 UKSim 14th International Conference on*, pp. 665-670, 2012.

[7] A. Aouaj, *et al.*, "Nanotube carbon transistor (CNTFET): I-V and C-V, a qualitative comparison between fettoy simulator and compact model," in *Multimedia Computing and Systems, 2009. ICMCS '09. International Conference on*, pp. 236-239, 2009.

[8] "FETToy numerical simulator," https://nanohub.org/resources/2844.

[9] A. Raychowdhury, *et al.*, "A circuit-compatible model of ballistic carbon nanotube field-effect transistors," *Computer-Aided Design of Integrated Circuits and Systems, IEEE Transactions on,* vol. 23, pp. 1411-1420, 2004.

[10] F. Pregaldiny, *et al.*, "Compact Modeling and Applications of CNTFETs for Analog and Digital Circuit Design," in *Electronics, Circuits and Systems, 2006. ICECS '06. 13th IEEE International Conference on*, pp. 1030-1033, 2006.

[11] G. Gelao, *et al.*, "A Semiempirical SPICE Model for n-Type Conventional CNTFETs," *Nanotechnology, IEEE Transactions on,* vol. 10, pp. 506-512, 2011.

[12] Subhajit Das, *et al.*, "Design of Digital Logic Circuits using Carbon Nanotube Field Effect Transistors," *International Journal of Soft Computing and Engineering (IJSCE),* vol. 1, p. 6, 2011.

[13] A. Mouatsi, *et al.*, "Effect of Subbands Energy in the CNTFET Characteristic's for Different Nanotube Diameter," *International Review of Physics,* vol. 6, pp. 68-72, 2012.

[14] J.-M. Park, *et al.*, "Comparison of simulation models for the coaxially-gated carbon-nanotube field-effect transistor," *Journal of the Korean Physical Society,* vol. 61, pp. 410-414, 2012/08/01, 2012.

[15] T. M. Abdolkader and M. A. Alam, "Diameter-dependent analytical model for light spot movement in carbon nanotube array transistors," *Applied Physics Letters,* vol. 98, p. 063503, 2011.

[16] A. Rahman, *et al.*, "Theory of ballistic nanotransistors," *Electron Devices, IEEE Transactions on,* vol. 50, pp. 1853-1864, 2003.

[17] R. Marani and A. G. Perri, "CNTFET Modelling for Electronic Circuit Design," *ECS Transactions,* vol. 23, pp. 429-437, September 4, 2009.